DOCKING OF SYNTHESIZED COMPOUNDS

6.1. Docking for EGFR TK interactions

In the MTT assay studies, a number of compounds showed very good inhibition. The compounds were structurally similar to gefitinib and other EGFR TKIs. Therefore, it was decided to explore the possible mechanism of action as EGFR kinase inhibition. The cell growth inhibition was observed in A-549, HCT-116 and MiaPaCa-2 cell lines, which are well known for EGFR over expression, it substantiated the consideration to check the EGFR kinase inhibition via docking studies.

6.2 Methodology

6.2.1 Docking protocol

Docking with Glide:

Protein preparation wizard of Maestro was used to prepare protein. The prepared protein was considered as an input file to generate receptor grid file, which was used further as input file for docking simulation. Grid of active sites were created using Maestro [80]. A centroid at 8.0, 6.0, 25.0 on x, y, z axis respectively was used to define the grid box. Grid box length was set to 6, 14 and 10 Å along x, y and z directions respectively. Ligand preparation was performed using "LigPrep" module of Schrodinger Suite 2013. LigPrep is used to create a single, low-energy, 3D structure with best chirality for each input structure. LigPrep can also produce specified number of structures from each input structure with numerous ionization states, stereo-chemistries, tautomers, and ring conformation. It eliminates molecules using given criteria including molecular weight or specified numbers and functional groups present. All the compound structures prepared with ligand preparation wizard of Maestro [81]. The ionization states in a given pH range of 7 ± 2 were produced by adding or removing protons from the ligand using EPIK 2.1 module [82]. For energy minimization OPLS 2005 Force Field was used. Different modules of Schrödinger suite were used during docking simulation and potential of non-polar parts of ligands were softened by scaling Vander Waals radii of ligand atoms by 0.8 Å with partial charge cut-off of 0.15. Glide first places the centre of ligand at various grid positions of a 1 Å grid during docking simulation, alter by rotating ligand in all the Euler angles it generates various possible conformations which has to pass through a filter series composed of initial rough positioning followed by scoring phase. The docking simulation was performed by

allowing flexible torsions in ligands with the use of XP mode. The parameter selected for docking run was kept default and a model energy function named as Glide score (Gscore) is used as output. Gscore combines force field and empirical terms for selecting the best docking pose was generated. Further docking simulations output file, having all the thermodynamics information such as Glide score, was analyzed using Glide XP visualizer, which enables visualization of ligand-receptor interactions in an interactive manner.

6.2.2 Oral Bioavailability Prediction

Prediction of oral bioavailability is very crucial to select the promising compounds which could be further optimized and it helps to identify potential candidates for clinical trials. Physicochemical properties such as molecular weight, hydrogen bond donor (HBD) count and hydrogen bond acceptor count (HBA), topological polar surface area (TPSA), molar refractivity (MR), and log partition coefficient (ClogP), which influence oral bioavailability were determined using Chemaxon Jchem for Excel.

Number of oxygen or nitrogen atoms with at least one hydrogen attached is defined as HBD, whereas HBA is defined as number of oxygen and nitrogen atoms present in the molecule bearing one lone pair of electrons. Total sum of polar atom surfaces in the molecule is defined as TPSA [83]. MR is the measure of total polarizability of a mole of a substance and LogP is octanol and water partition coefficient. All these parameters affect compound solubility, partitioning between biological barriers and system which can have direct correlation with oral bioavailability. Based on observation of approved drugs with these properties various rules have been developed to predict oral bioavailability. One such rule is Rule of five or Lipinsky rule, which states that for good oral bioavailability any molecule should not violate more than one of the following rules [84].

a. LogP should be less than 5.

b. Molecular weight should be less than 500 kDa.

c. Should have less than 5 hydrogen bond donors (sum of hydroxyl and amine groups).

d. Should have less than 10 hydrogen-bond acceptors (sum of oxygen and nitrogen atoms).

6.2.3 Toxicity Prediction

Toxicity prediction of chemical structure before animal studies can provide valuable information and reduces animal usage in screening. Risk of elimination of potential compound at the later phase of clinical development can also be reduced by early prediction of toxicity. All compounds should hence be tested for biological safety/ toxicity in order to minimize the later elimination. Common toxicity screening tests involve study of tumorogenicity, mutagenicity, reproductive toxicity, skin irritation, cardiotoxicity, etc. In this study, the toxicity risk assessment was carried using OSIRIS property explorer, a software of Actelion Pharmaceuticals Ltd., Switzerland, hosted on http://www.organic-chemistry.org website [85] [86].

Drug likeliness score involves physicochemical properties and functional groups present in available marketed drugs. It is defined as a overall balance of various molecular properties and structural features which determine whether given molecule is similar to the known drugs or not. These properties, mainly include hydrophobicity, hydrogen bonding, electronic distribution, molecule size and flexibility [87]. Various pharmacophoric features which affect the bioavailability are distribution, affinity to proteins or receptor, reactivity, metabolic stability and toxicity in biological system. Drug score is a measure of toxicity risk and drug likeliness score. Drug likeliness should be a positive value and higher the values more the pharmacokinetic similarity with ideal drug. The Drug score is calculated from partition coefficient, logS (solubility) and molecular weight, Whereas drug likeness takes into account the drug score along with risk factors. (Some parameters accessed from http://www.molinspiration.com/cgi-bin/properties, http://molsoft.com/mprop/) [88] .

6.3 Selection and validation of 3D crystal structure of EGFR

Several 3D crystallographic structures of EGFR along with ligand have been reported in protein data bank. PDB structure 2ITO was selected. It has resolution of 3.25 A^0. The docking process using 2ITO was validated using extracted ligand (gefitinib). The validation of docking protocol is essential to ensure reliability and reproducibility of docking parameters used for given study protocol [89].

The docked ligand superimposed well on the reference ligand (co-crystallized ligand) with RMSD value of 0.458 with glide score of -7.3 (Figure 6.1). The docked ligand also displayed

hydrogen bonding interactions with amino acids MET793 and other hydrophobic interactions are with LEU844, MET766, CYS797, ALA743, LEU792 etc.

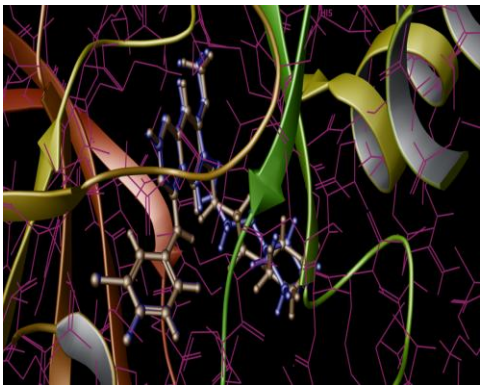

(A)

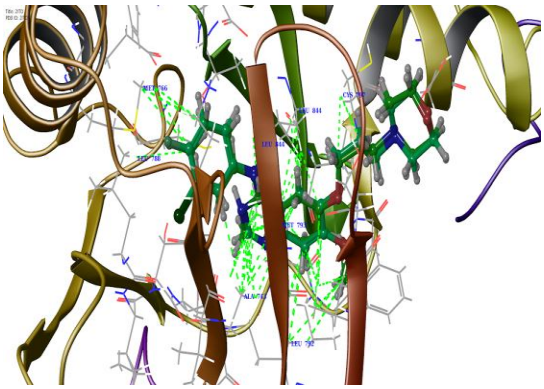

(B)

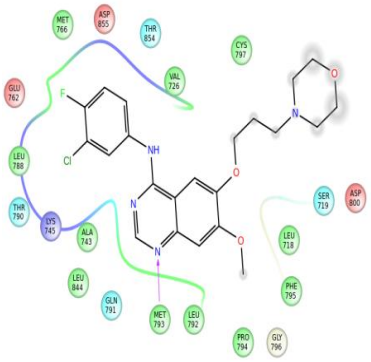

(C)

Figure 6.1: Docking validation (A) Redocked pose of gefitinib superimposed with the co-crystallized ligand (B) Various interactions of redocked ligand (C) 2D interaction plot of gefitinib in active site of 2ITO

6.4 Docking results and discussion

Epidermal growth factor receptor is cell surface receptor and phosphorylation takes place with the help of tyrosine kinase of kinase family. After validation all the compounds were docked in the active cite, kinase region of receptor and the discussion is summarized below as scaffold wise.

6.4.1 [4-(benzyloxy)phenyl](4-benzylpiperazin-1-yl)methanone derivatives (scaffold-I)

The Glide score of compounds in this series is given in table 6.1

Table 6.1 *In silico* docking results of compounds of scaffold I

Code No	R	Glide Score (kcal/mol)
A-1	2-Cl	-5.98
A-2	4-Cl	-5.79
A-3	2-F	-6.13
A-4	4-F	-6.32
A-5	2-NO_2	-6.21
A-6	2-OCH_3	-5.89
A-7	3-OCH_3	-6.25
A-8	4-OCH_3	-6.79
A-9	2,3-diCl	-6.12
A-10	2-CH_3	-6.33
A-11	3-CH_3	-5.79
A-12	4-CH_3	-6.48

Piperazine derivatives have been reported to have anticancer activity [90]. Among electron withdrawing group substituted compounds, compound A-8 showed the best glide score. All compounds A-1 to A-4 showed hydrogen bonding with MET793 of the hinge region. These compounds also showed the hydrophobic interactions with GLY796, LEU792, LEU844, CYS797, ASP800 or ASP855. Compound A-9 with 2,3-diCl substitution also resulted in similar glide score and showed hydrogen bonding with MET793 as well as hydrophobic interactions with above amino acids. Nitro substituted compound (A-5) was devoid of hydrogen bonding interactions with MET793 of hinge region but it retained all hydrophobic interactions having THR790 as extra hydrophobic interaction. When compounds were substituted with -OCH3, compound A-8, and A-7 with para methoxy and meta substitution showed better glide score as both showed MET793 hydrogen bonding of hinge region whereas A-6 was devoid of hydrogen bonding

interaction with MET793. All hydrophobic interactions were same for both of the compounds. Among A-10 to A-12, A-11 was devoid of hydrogen bonding thus resulted with lesser glide score when compared with A-10 and A-12.

Compound A-8 and A-10 showed very well correlated glide score within their cell line inhibition as A-8 showed less than 10 µM IC_{50} in MIAPaCa-2 cell line whereas A-10 showed best inhibition in HCT-116 colon cancer line among all compounds.

For better EGFR inhibition, additional hydrogen / covalent bonding with CYS797 and ASP800 or ASP855, THR854 and ASP855 are also required and it was not observed with any of the compounds.

Some 2D and 3D interaction of representative compound are given in Figure 6.2

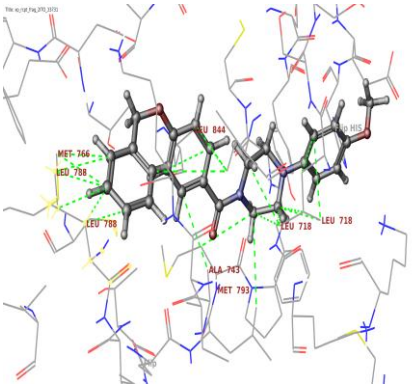

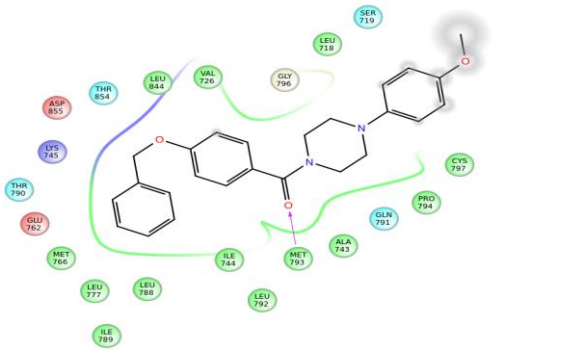

3D interaction diagram of A-8

2D ligplot of A-8

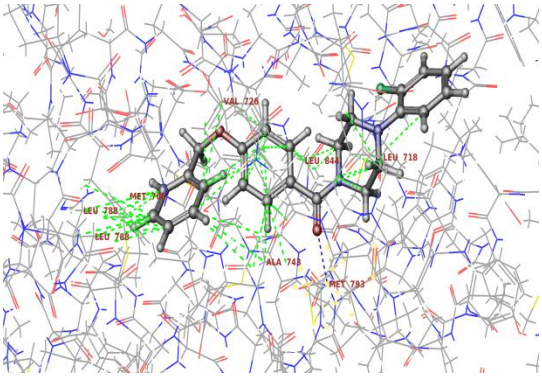

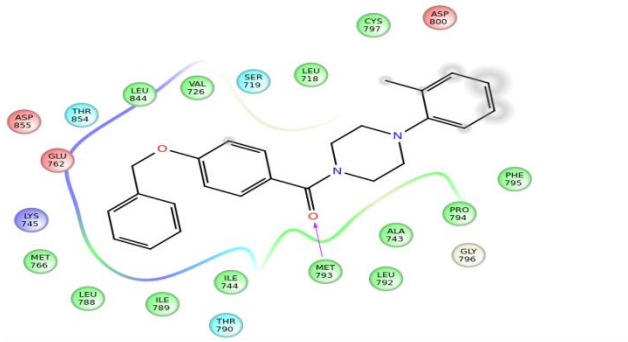

3D interaction diagram of A-10

2D ligplot of A-10

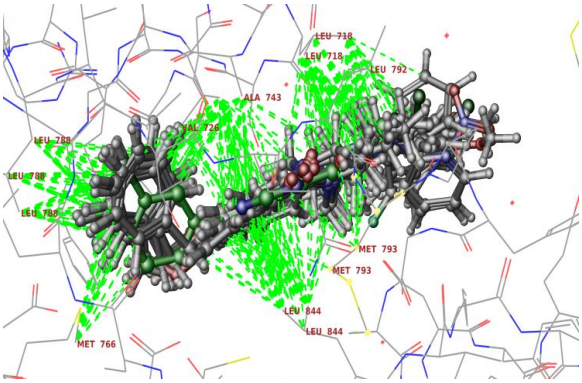

Overlay of all the Compounds of scaffold I in active site

Figure 6.2: Docking poses of representative substituted [4-(benzyloxy)phenyl](4-benzylpiperazin-1-yl)methanone series derivatives

Oral bioavailability prediction:

All compounds were very well within the criteria of Lipinski rule. The log P values were in the range of 2 to 5.5. Hydrogen bond donor and acceptor count also followed the Lipinski rule. All compounds in the series were predicted to not have any mutagenic, tumorogenic property but showed positive potential for kinase inhibition property.

Table 6.2 *In silico* physiochemical property results of compounds of scaffold I

Code No	R	MW	HBA	HBD	PSA	LogP	AMES toxicity	Carcino gecity	Drug likeliness	KI
A-1	*2*-Cl	406.91	3	0	27.06	4.88	No	No	0.00	Yes
A-2	*4*-Cl	406.91	3	0	27.33	4.88	No	No	0.01	Yes
A-3	*2*-F	390.45	3	0	27.07	4.36	No	No	-0.19	Yes
A-4	*4*-F	390.45	3	0	27.07	4.36	No	No	-0.37	Yes
A-5	*2*-NO_2	417.25	5	0	65.03	4.13	Yes	No	-0.37	Yes
A-6	*2*-OCH_3	402.23	4	0	34.70	4.23	No	No	-0.27	Yes
A-7	*3*-OCH_3	402.25	4	0	34.92	4.23	No	No	-0.24	Yes
A-8	*4*-OCH_3	402.25	4	0	34.92	4.23	No	No	-0.57	Yes
A-9	*2,3*-diCl	441.23	3	0	27.07	5.41	No	No	0.27	Yes
A10	*2*-CH_3	386	3	0	27.37	4.53	No	No	-0.47	Yes

A-11	*3*-CH_3	386.49	3	0	27.37	4.53	No	No	-0.47	Yes
A-12	*4*-CH_3	386.49	3	0	27.07	4.53	No	No	0.00	Yes

6.4.2 4-(3-(4-methylpiperazin-1-yl)propoxy)-N-phenylbenzamide (scaffold-II) and (4-(3-methoxyphenyl)piperazin-1-yl)(4-(3-(4-methylpiperazin-1-yl)propoxy)phenyl)methanone derivatives (scaffold-III)

Glide score of compounds are given below in the table 6.3

Table 6.3: *In silico* docking results of compounds of scaffold II and III

Code	R	Glide Score (kcal/mol)
Aniline substituent's (scaffold-II)		
B-1	H	-6.55
B-2	4-CH_3	-6.53
B-3	3-CH_3	-5.93
B-4	2,4 di-CH_3	-6.25
B-5	3,4 di-CH_3	-6.11
B-6	2,5 di-CH_3	-6.79
B-7	4-OCH_3	-7.07
B-8	4-Cl	-5.18
B-9	4-Br	-6.31
B-10	4-F	-5.84
Piperazine Substituent's (scaffold-III)		
B-11	3-OCH_3	-7.03
B-12	4-OCH_3	-7.07
B-13	2-Cl	-6.69
B-14	4-Cl	-6.59
B-15	2,3-diCl	-7.49
B-16	4-CH_3	-5.29

In this series morpholine of gefitinib was replaced with *N*-methyl piperazine and quinazoline with amide group. Amide compounds have been reported as EGFR TK inhibitors [72].

Among all anilines with electron donating groups (B-1 to B-6), only B-6 with 2,5 di-CH_3 substitution showed hydrogen bonding interaction with MET793 of hinge region and resulted in highest glide score. Hydrophobic interactions were similar for all compounds with CYS797, LEU792 and MET793 of hinge region, LEU844 and MET766 in the C-helix. Additionally B-6 had side chain hydrogen bonding with ASP855 in activation loop.

Among electron withdrawing substituents, B-8 (Cl), B-9 (Br) and B-10 (F), B-9 showed the highest glide score which is rationalized by its hydrogen bonding with MET793 of hinge region. Hydrophobic interactions were similar for all compounds with CYS797, THR790, LEU792 and MET793 of hinge region and LEU844 and MET766 in the C-helix. Compound B-7 with 4-OCH_3 group also showed hydrogen bonding interaction with MET793 and side chain hydrogen interaction with ASP855 in activation loop hence resulted in improved glide score.

In piperazine substituted compounds, B-11 (3-OCH_3) and B-12 (4-OCH_3) showed similar dock scores but were devoid of hydrogen bonding with MET793. However all required hydrophobic interactions with CYS797, THR790, LEU792 and MET793 of hinge region, LEU844 in activation loop, and MET766 in the C-helix were present. Both the compounds showed side chain hydrogen interaction with ASP800.

Introduction of 2-chloro (B-13) and 2,3 dichloro (B-15) on phenyl piperazine resulted in hydrogen bonding of MET793. Ionic interaction with ASP800 and hydrophobic interactions with CYS797 and LEU792 of hinge region, LEU844, and MET766 in the C-helix were retained by both the compounds. Chloro at para position (B-14) of phenyl piperazine did not show hydrogen bonding with MET793 hence, resulted in less glide score as compared to B-13 (2-Cl) and B-15 (2,3-Cl). Methyl substituent at para position resulted in decreased dock score as it did not show hydrogen bonding with MET793 although, it retained all desired hydrophobic interactions. No compound had MET793 and CYS797 or any other hydrogen bonding interactions, which is required for EGFRTK inhibition.

When the best glide score compounds (scaffold-II) were compared with their IC_{50} values, the best glide score is of compound B-6 and the compound shows comparable inhibition to gefitinib in all three cell lines.

Compounds with scaffold-III, such as B-11 (3-OCH_3) and B-12 (4-OCH_3) resulted in good glide scores and the IC_{50} value of B-11 (3-OCH_3) was better than gefitinib in all three cell lines. Although B-15 had best glide score in the series, it was devoid of inhibition. B-16 showed poor glide score but resulted in the comparative inhibition to gefitinib.

Oral bioavailability prediction

All designed compounds were very well within the criteria of Lipinski rule. The log P values were within range of 2 to 4. Hydrogen bond donor between 4-7 and acceptor count was less than 2 followed the Lipnski rule. Polar Surface Area (PSA) for all compounds was found to in limit below 140A^0 hence BBB permeability for the series was predicted to be good. All compounds in the series were predicted to be devoid of mutagenic and tumorogenic property. Kinase inhibition was positive for all designed compounds. Drug likeliness scores were also good for compounds.

Table 6.4 *In silico* physiochemical property prediction of compounds of scaffold II and III

Code	R	MW	HBA	HBD	PSA	LogP	AMES toxicity	Carcinogecity	DL	KI
Aniline substituent's (scaffold-II)										
B-1	H	353.46	4	1	37.93	2.95	No	No	2.06	Yes
B-2	p-CH_3	367.49	4	1	37.93	3.26	No	No	1.94	Yes
B-3	m-CH_3	367.49	4	1	37.93	3.26	No	No	1.77	Yes
B-4	2,4 di-CH_3	381.52	4	1	37.24	3.57	No	No	1.55	Yes
B-5	3,4 di-CH_3	381.52	4	1	37.93	3.57	No	No	1.42	Yes
B-6	2,5 di-	381.52	4	1	37.93	3.57	No	No	1.99	Yes

	CH_3									
B-7	p-OCH_3	383.49	5	1	45.48	2.96	No	No	1.94	Yes
B-8	p-Cl	387.91	4	1	37.93	3.62	Yes	No	2.42	Yes
B-9	p-Br	432.36	4	1	43.86	3.72	No	No	0.53	Yes
B-10	p-F	371.45	4	1	37.93	3.09	No	No	2.25	Yes
Piperazine substituent's (scaffold-III)										
B-11	3-OCH_3	452.56	6	0	42.30	2.67	No	No	1.32	Yes
B-12	4-OCH_3	452.56	6	0	42.30	2.67	No	No	1.16	Yes
B-13	2-Cl	457.15	5	0	34.45	3.31	No	No	1.52	Yes
B-14	4-Cl	443.97	5	0	35.55	3.31	No	No	1.53	Yes
B-15	2,3-diCl	491.63	5	0	34.45	3.97	No	No	1.72	Yes
B-16	4-CH_3	436.6	5	0	34.75	2.97	No	No	1.20	Yes

2D and and 3D interaction pose of representative compounds from scaffold-III and IV are given in Figure 6.3.

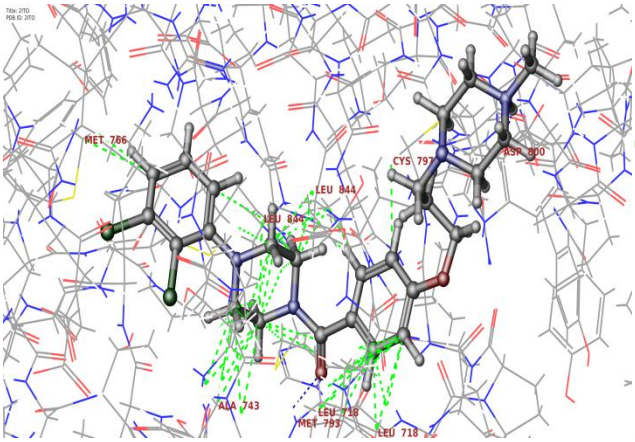

3D interaction diagram of B-15

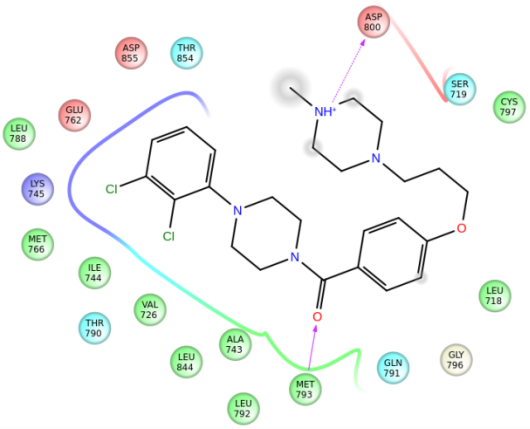

2D ligplot of B-15

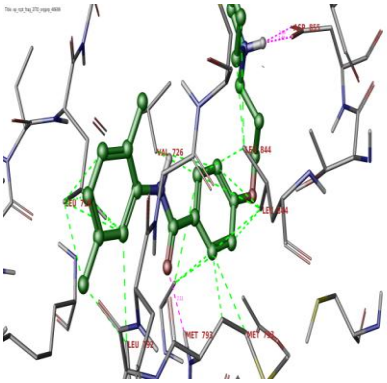

3D interaction diagram of B-6

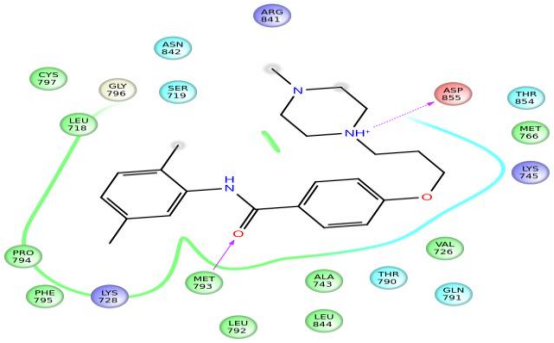

2D ligplot of B-6

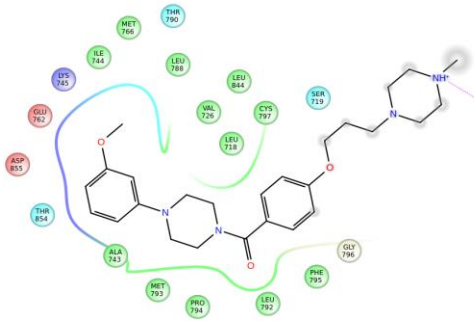

2D ligplot of B-11

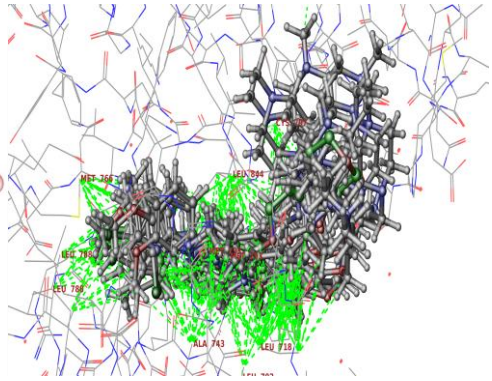

Overlay of all compounds in active site

Figure 6.3: 2D and 3D active site interactions of some representative compounds of scaffold II and III

6.4.3 4-(3-(4-ethylpiperazin-1-yl)propoxy)-N-phenylbenzamide (scaffold-IV) and (4-(3-(4-ethylpiperazin-1-yl)propoxy)phenyl)(4-(2-methoxyphenyl)piperazin-1-yl)methanone derivatives (scaffold-V) as EGFRTK inhibitors

Glide score of compounds are given below in the table 6.5

Table 6.5**:** *In silico* docking results of compounds of scaffold IV and V

Code	R	Glide Score (kcal/mol)
Aniline substituent's (scaffold-IV)		
C-1	H	-6.12
C-2	4-CH_3	-5.75
C-3	3-CH_3	-5.55

C-4	2,4 di-CH_3	-6.68
C-5	3,4 di-CH_3	-5.97
C-6	2,5 di-CH_3	-7.43
C-7	4-OCH_3	-7.06
C-8	4-Cl	5.55
C-9	4-Br	-5.76
C-10	4-F	-5.78
Piperazine substituent's (scaffold-V)		
C-11	3-OCH_3	-5.28
C-12	4-OCH_3	-5.31
C-13	2-Cl	-6.15
C-14	4-Cl	-6.13
C-15	2,3-diCl	-6.43
C-16	4-CH_3	-6.58

From compounds C-1 to C-7 (anilines) with electron donating substituent, only C-6 (2,5 di-CH_3) and C-7 (4-OCH_3) showed hydrogen bonding interactions with MET793. Highest glide score was for C-6 (2,5 di-CH_3) and it showed side chain hydrogen bond interaction with THR854 and ionic interactions with ASP855 and GLU762. Compounds C-1 to C-5 showed side chain hydrogen bonding interaction with ASP855 and retained the desired hydrophobic interactions. All the compounds showed hydrophobic interactions with CYS797, LEU792 of hinge region, LEU844 activation loop, and MET766 in the C-helix. Electron withdrawing substituted compounds such as C-8 (4-Cl), C-9 (4-Br) and C-10 (4-F) did not show hydrogen bonding with MET793 and were also devoid of side chain hydrogen interaction, also hence poor glide scores obtained.

In piperazine series of compounds, electron donating group substituted compounds C-11 (3-OCH_3) and C-12 (4-OCH_3) did not show hydrogen bonding with MET793 and even were devoid of side chain hydrogen bond interactions. However both these compounds, showed all hydrophobic interactions.

Compounds with electron withdrawing substituents in piperazine series, C-13 (*2*-Cl), C-14 (*4*-Cl) and C-15 (*2,3*-Cl) showed hydrogen bonding with MET793, ionic interaction with ASP800 and also maintained all other hydrophobic interactions. No compound showed more than two back bone hydrogen bonds which could impart them better EGFRTK inhibition.

Among the scaffold IV compounds, compound C-6 and C-7 resulted in the best glide score but did not result in good inhibition. Compound C-4 with a glide score of -6.68 resulted in IC_{50} value of 11.33 in colon cancer cell line which is comparable to gefitinib whereas, compound C-2 has poor glide score but showed better IC_{50} value than gefitinib in MIAPaCa-2 cell line.

From scaffold V series, best active compound was C-14 with a glide score -6.13, and it showed IC_{50} value of less than 1μM.

Oral bioavailability prediction

All designed compounds were very well within in the criteria of Lipinski rule. The log P values were in the range of 2 to 5. Hydrogen bond donor and acceptor count followed the Lipinski rule. Polar surface area (PSA) for all compounds was found to be below 140 A^0. All compounds in the series were predicted to lack mutagenic and tumorogenic potential. Kinase inhibition was predicted to be positive for all compounds. Drug likeliness scores were also good.

In silico physiochemical property prediction of Phenyl-4-[3-(4-ethylpiperazin-1-yl)propoxy] benzamide derivatives are also given below in table 6.6. 2D and 3D interaction interactions of some representative compounds from Phenyl-4-[3-(4-ethylpiperazin-1-yl)propoxy] benzamide series are given in Figure 6.4

Table 6.6 *In silico* physiochemical property prediction of compounds of scaffold IV and V

Code	R	MW	HBA	HBD	PSA	LogP	AMES toxicity	Carcinogecity	Drug likeliness	KI
Aniline substituent's (scaffold-IV)										
C-1	H	367.493	4	1	38	3.34	No	No	1.93	Yes
C-2	p-CH_3	381.52	4	1	38	3.62	No	No	1.84	Yes
C-3	m-CH_3	381.52	4	1	38	3.65	No	No	1.66	Yes

C-4	2,4 di-CH_3	395.54	4	1	37.30	3.96	No	No	1.44	Yes
C-5	3,4 di-CH_3	395.54	4	1	38.00	3.96	No	No	1.31	Yes
C-6	2,5 di-CH_3	395.54	4	1	38.00	3.96	No	No	1.88	Yes
C-7	p-OCH_3	397.51	5	1	45.54	3.35	No	No	1.83	Yes
C-8	p-Cl	401.93	4	1	38.00	3.99	No	No	2.31	Yes
C-9	p-Br	446.38	4	1	38.00	4.10	No	No	2.01	Yes
C10	p-F	385.48	4	1	38.00	3.48	No	No	2.14	Yes
Piperazine substituent's (scaffold-V)										
C-11	3-OCH_3	466.3	6	0	42.36	3.06	No	No	1.20	Yes
C-12	4-OCH_3	466.3	6	0	42.36	3.06	No	No	1.04	Yes
C-13	2-Cl	471.04	5	0	34.51	3.70	No	No	1.39	Yes
C-14	4-Cl	471.04	5	0	34.81	3.70	No	No	1.40	Yes
C-15	2,3-diCl	505.49	5	0	34.51	4.36	No	No	1.60	Yes
C-16	4-CH_3	452.32	5	0	43.86	3.12	No	No	0.53	Yes

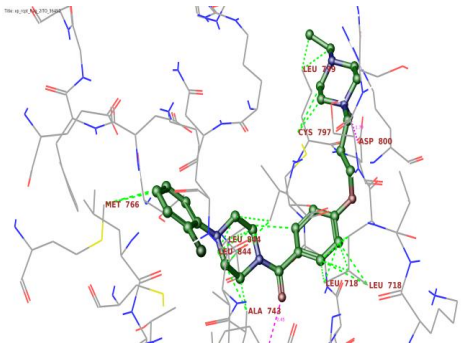

3D interaction diagram of C-13

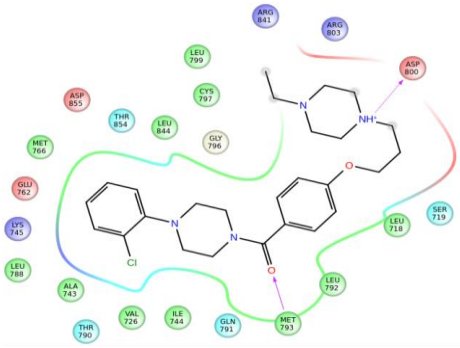

2D ligplot of C-13

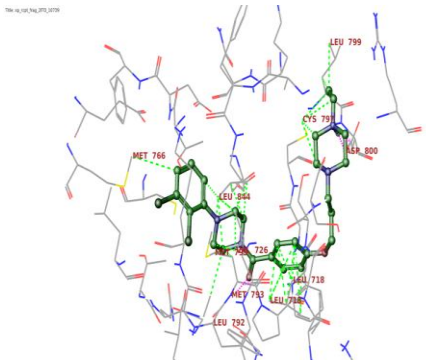

3D interaction diagram of C-15

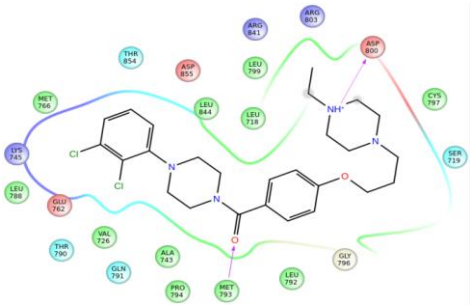

2D ligplot of C-15

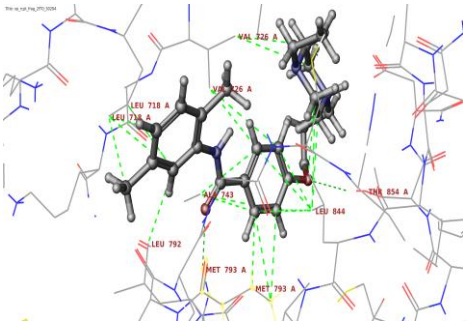

3D interaction diagram of C-6

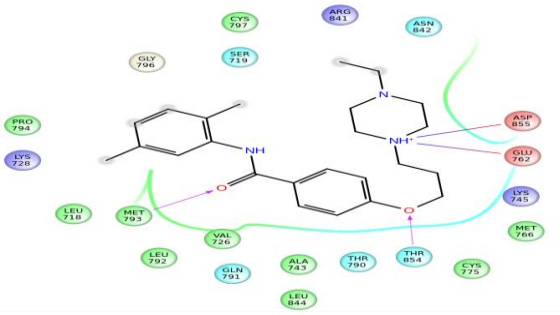

2D ligplot of C-6

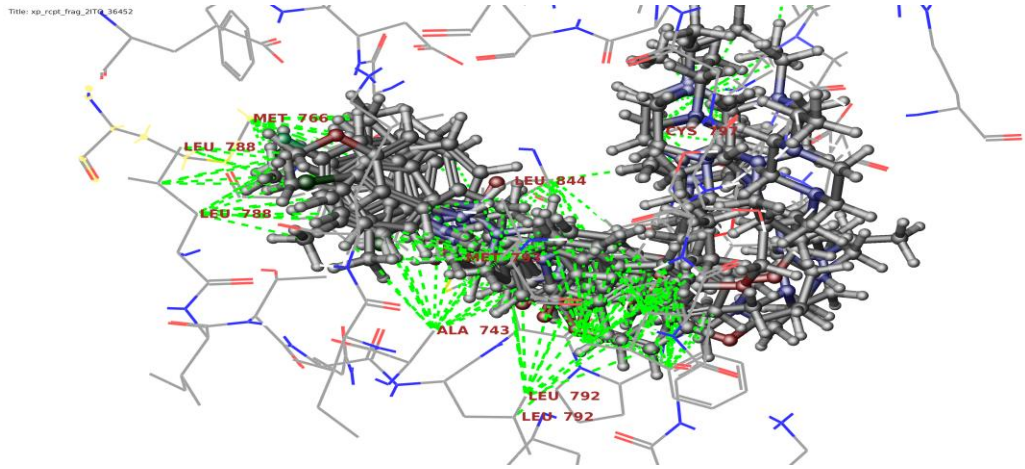

Overlay in active site

Figure 6.4: 2D and 3D interaction of some representative compounds of scaffold IV and V

6.4.4 4-[3-(morpholin-4-yl)propoxy]-*N*-phenylbenzamide derivative(scaffold-VI) and (4-(2-methoxyphenyl)piperazin-1-yl)(4-(3-morpholinopropoxy)phenyl)methanonederivatives (scaffold-VII)

Glide score of compounds from this series are given below in the table 6.7

Table 6.7: *In silico* docking results of compounds of scaffold VI and VII

Code no.	R	Glide Score (kcal/mol)
Aniline substituent's (scaffold-VI)		
D-1	H	-6.185
D-2	4-CH_3	-7.105
D-3	3-CH_3	-5.942
D-4	2,4 di-CH_3	-7.149
D-5	3,4 di-CH_3	-7.04
D-6	2,5 di-CH_3	-6.70
D-7	4-OCH_3	-7.16
D-8	4-Cl	-7.17
D-9	4-Br	-5.64-
D-10	4-F	-6.23
D-11	2-Cl	-6.80
Piperazine substituent's (scaffold-VII)		
D-12	2-OCH_3	-6.86
D-13	3-OCH_3	-5.90
D-14	4-OCH_3	-6.59
D-15	2-Cl	-6.21
D-16	4-Cl	-6.69
D-17	2,4-diCl	-6.43

D-18	2-F	-5.96
D-19	4-CH_3	-5.48
D-20	4-NO_2	-7.21

Among the aniline derivatives, D-1 (H) showed hydrogen bonding with only CYS797. Hydrophobic interactions were with CYS797 and LEU792 residue of hinge region and with LEU844, and MET766 in the C-helix.

Introduction of methyl group at 4thposition (D-2) resulted in hydrogen bonding interaction with MET793 and side chain hydrogen interaction with SER719, hence showed improved glide score, whereas 3-methyl was devoid of hydrogen bonding interaction. Both the compounds showed desired hydrophobic interactions. Out of D-4 (*2,4 di*-CH_3) D-5 (*3,4 di*-CH_3) and D-6 (*2,5 di*-CH_3), D-4 and D-5 showed hydrogen bonding with MET793 of hinge region, side chain hydrogen bonding with ASP800, whereas D-6 did not show hydrogen bonding. Rest hydrophobic interactions were same for all. D-7 also shows hydrogen bonding with MET793 and side chain hydrogen bonding interaction with ASP855.

Out of D-8 (*4*-Cl), D-9 (*4*-Br) and D-10 (*4*-F), both D-8 and D-10 showed hydrogen bonding with MET793. Additionally, D-8 also showed side chain hydrogen interaction with ASP855 hence showed highest glide score among all three.

Among piperazine substituted compounds D-12 (*2*-OCH_3), D-13 (*2*-OCH_3) and D-14(*2*-OCH_3), D-12 and D-14 shows hydrogen bonding interaction with MET793 along with side chain hydrogen interaction with ASP800. Compounds with electron withdrawing halogens D-15 (*2*-Cl), D-16 (4-Cl), D-17 (2,4 di-Cl), D-18 (*2*-F) and D-16 (4-Cl) resulted in highest glide score as it retained hydrogen bonding with MET793, PHE723 and side chain hydrogen interaction with LYS745. Rest all compounds were devoid of hydrogen bond interactions although all the hydrophobic interactions were present.

Most prominent interactions were present in D-20 (NO_2) and include ionic interactions with GLU762 and LYS745, hydrogen bonding with GLY796, MET793 and also LYS745 and side chain

hydrogen interaction with ASP800. In this series D-20 has more than two hydrogen bonds however it did not show any interaction with CYS797.

From the scaffold VI, D-2, D-4, D-5 and D-7 showed MET793 hydrogen bonding hence resulted in improved glide scores. D-4 and D-5 showed the best IC_{50} values in MIAPaCa-2 and HCT-116 cell lines.

Among scaffold VII compounds, compound D-16 with a glide score of -6.69 resulted in best inhibition value in all three cell lines. Although compound D-20 showed the maximum interactions and good glide score, it was not active in MTT assay.

Oral bioavailability and toxicity prediction:

All designed compounds were very well within in the criteria of Lipinski rule. The log P values were in the range of 2 to 5 and hydrogen bond donor count, hydrogen bond acceptor count was from 4 to 6. All ligands had polar surface area less than 70 A^0 and hence BBB permeability for the series was predicted to be good. All compounds in the series were predicted to have negative mutagenic and tumorogenic potential. However, kinase inhibitory potential was positive.

I*n silico* physiochemical property prediction of 4-[3-(morpholin-4-propoxy]-N-amides derivatives are given below in table 6.8

Table 6.8 In *silico* physiochemical property prediction of of scaffold VI and VII

Code no.	R	MW	HBA	HBD	PSA	LogP	AMES T	CN	DL	KI
Aniline substituent's (scaffold-VI)										
D-1	H	340.44	4	1	42.37	3.04	No	No	1.65	Yes
D-2	4-CH_3	354.45	4	1	42.37	3.34	No	No	1.65	Yes
D-3	3-CH_3	354.45	4	1	42.37	3.34	No	No	1.50	Yes
D-4	2,4 di-CH_3	368.47	4	1	41.67	3.34	No	No	1.80	Yes
D-5	3,4 di-CH_3	368.47	4	1	41.67	3.80	No	No	1.31	Yes
D-6	3,5 di-CH_3	368.47	4	1	41.67	3.80	No	No	1.42	Yes
D-7	4-OCH_3	339.56	4	1	42.67	3.80	No	No	1.70	Yes

D-8	4-Cl	374.35	4	1	42.37	3.69	No	No	2.02	Yes
D-9	4-Br	418.09	4	1	42.37	3.97	No	No	1.73	Yes
D-10	4-F	358.41	4	1	42.37	3.17	No	No	1.86	Yes
D-11	2-Cl	374.86	4	1	41.67	3.71	No	No	1.87	Yes
Piperazine substituent's (scaffold-VII)										
D-12	2-OCH_3	439.25	6	0	46.51	3.07	No	No	0.90	Yes
D-13	3-OCH_3	439.25	6	0	46.73	3.19	No	No	1.07	Yes
D-14	4-OCH_3	439.25	6	0	46.73	3.19	No	No	0.90	Yes
D-15	2-Cl	443.97	5	0	38.88	3.40	No	No	1.16	Yes
D-16	4-Cl	443.97	5	0	39.18	3.81	No	No	1.14	Yes
D-17	2,4-diCl	477.16	5	0	38.88	4.29	No	No	1.38	Yes
C-18	2-F	427.23	4	0	38.88	3.25	No	No	1.01	Yes
D-19	4-CH_3	423.25	4	0	38.88	3.38	No	No	1.23	Yes
D-20	4-NO_2	454.25	6	0	40.88	2.65	No	No	0.66	Yes

2D and 3D interaction interactions of some representative compounds from this series are given in Figure 6.5.

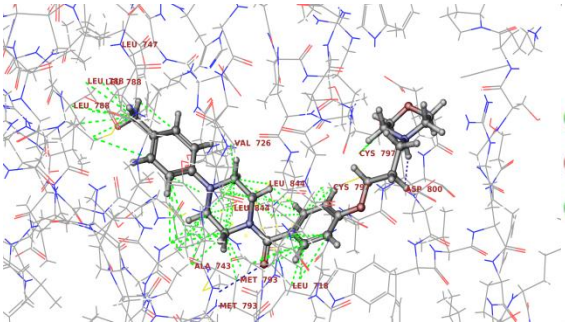

3D interaction diagram of D-2

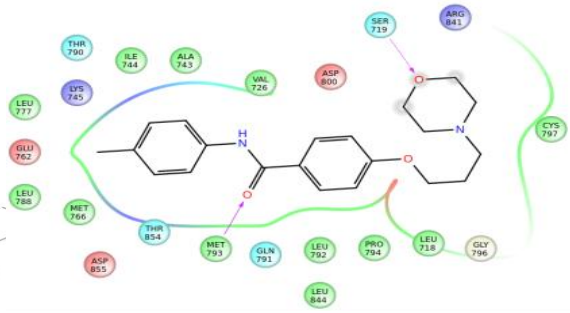

2D ligplot of D-2

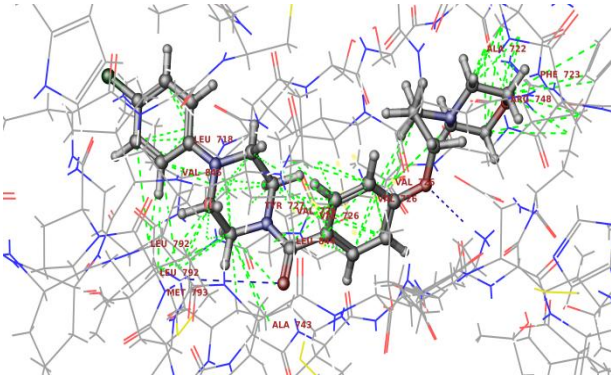

3D interaction diagram of D-8

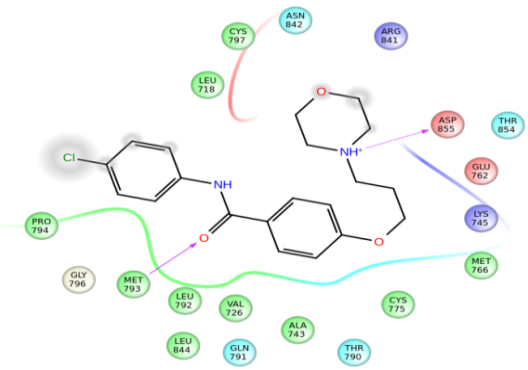

2D ligplot of D-8

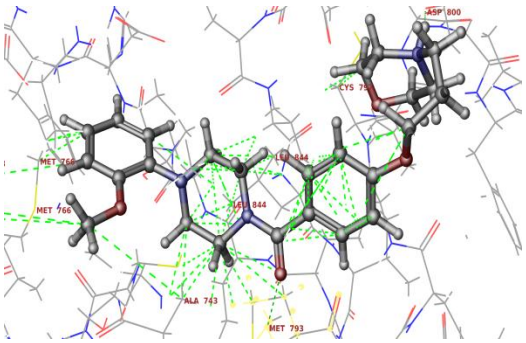

3D interaction diagram of D-12

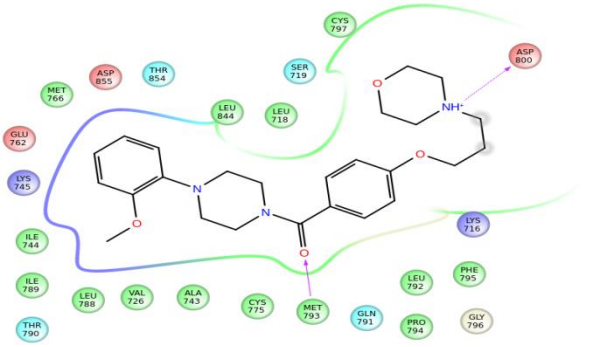

2D ligplot of D-12

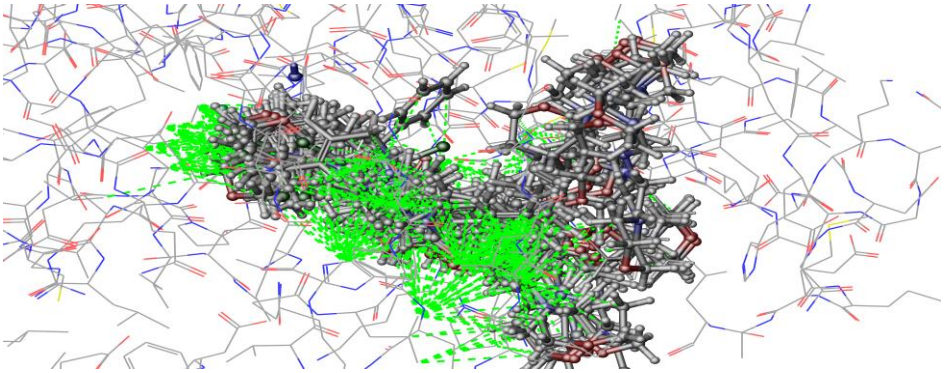

Overlay in active site

Figure 6.5: 2D and 3D interaction interactions of some representative compounds of scaffold VI and VII